Normal telomere length and chromosomal end capping in poly(ADP-ribose) polymerase–deficient mice and primary cells despite increased chromosomal instability

Enrique Samper,[1] Fermín A. Goytisolo,[1] Josiane Ménissier-de Murcia,[2] Eva González-Suárez,[1] Juan C. Cigudosa,[3] Gilbert de Murcia,[2] and María A. Blasco[1]

[1]Department of Immunology and Oncology, Centro Nacional de Biotecnología-CSIC, Campus Cantoblanco, E-28049 Madrid, Spain
[2]Centre National de la Recherche Scientifique, Laboratoire Conventionné avec le Commissariat à l´Energie Atomique, Ecole Superieure de Biotechnologie de Strasbourg, 67400 Illkirch-Graffenstaden, France
[3]Cytogenetics Unit, Centro Nacional de Investigaciones Oncologicas Carlos III, Majadahonda, E-28220 Madrid, Spain

Poly(ADP-ribose) polymerase (PARP)-1, a detector of single-strand breaks, plays a key role in the cellular response to DNA damage. PARP-1–deficient mice are hypersensitive to genotoxic agents and display genomic instability due to a DNA repair defect in the base excision repair pathway. A previous report suggested that PARP-1–deficient mice also had a severe telomeric dysfunction consisting of telomere shortening and increased end-to-end fusions (d'Adda di Fagagna, F., M.P. Hande, W.-M. Tong, P.M. Lansdorp, Z.-Q. Wang, and S.P. Jackson. 1999. *Nat. Genet.* 23: 76–80). In contrast to that, and using a panoply of techniques, including quantitative telomeric (Q)-FISH, we did not find significant differences in telomere length between wild-type and PARP-1$^{-/-}$ littermate mice or PARP-1$^{-/-}$ primary cells. Similarly, there were no differences in the length of the G-strand overhang. Q-FISH and spectral karyotyping analyses of primary PARP-1$^{-/-}$ cells showed a frequency of 2 end-to-end fusions per 100 metaphases, much lower than that described previously (d'Adda di Fagagna et al., 1999). This low frequency of end-to-end fusions in PARP-1$^{-/-}$ primary cells is accordant with the absence of severe proliferative defects in PARP-1$^{-/-}$ mice. The results presented here indicate that PARP-1 does not play a major role in regulating telomere length or in telomeric end capping, and the chromosomal instability of PARP-1$^{-/-}$ primary cells can be explained by the repair defect associated to PARP-1 deficiency. Finally, no interaction between PARP-1 and the telomerase reverse transcriptase subunit, Tert, was found using the two-hybrid assay.

Introduction

Poly(ADP-ribose) polymerase (PARP)-1* is a nuclear protein which is selectively activated by DNA strand breaks to catalyze the immediate addition of long-branched chains of poly(ADP-ribose) from NAD to a variety of nuclear proteins, including itself, influencing chromatin architecture and DNA transactions (for review see d'Amours et al., 1999; Bürkle et al., 2000). As a detector of single-strand breaks (Menissier-de Murcia et al., 1989), PARP-1 has been proposed to have an important role in base excision repair (Jeggo, 1998). Indeed, several knockout mice lacking the PARP-1 protein show hypersensitivity to genotoxic stress, as well as an increased chromosomal instability after DNA damage (Menissier-de Murcia et al., 1997; Beneke et al., 2000). PARP-1 also has been shown to play a role in (a) chromatin remodeling through its ability to modify histones (Poirier et al., 1982), (b) signaling DNA damage through polymer synthesis and/or its interaction with DNA-PKc's, ATM, and p53 (for review see Bürkle et al., 2000), (c) gene expression through its interaction with transcription factors and enhancers (Oei et al., 1997; Plaza et al., 1999), (d) the base excision repair pathway through its interaction with XRCC1 (Masson et al., 1998; Dantzer et al., 2000), as well as (e) apoptosis (D'Amours et al., 1998). Unexpectedly, genetic deletion of PARP-1 has revealed the instrumental role of PARP-1 in cell

Address correspondence to María Blasco, Department of Immunology and Oncology, Centro Nacional de Biotecnologia - CSIC, Campus Cantoblanco, E-28049 Madrid, Spain. Tel.: (34) 915-854-846; Fax: (34) 913-720-493. E-mail: mblasco@cnb.uam.es

E. Samper and F. Goytisolo contributed equally to this work.

*Abbreviations used in this paper: BM, bone marrow; MEF, mouse embryonic fibroblast; PARP, poly(ADP-ribose) polymerase; Q, quantitative telomeric; SKY, spectral karyotyping; TRF, terminal restriction fragment.

Key words: telomeres; PARP-1; telomerase; DNA repair; chromosomal stability

death after ischemia-reperfusion injury and in various inflammatory processes (for review see Pieper et al., 1999).

The ends of chromosomes consist of a special structure termed the telomere. Telomeres have an essential role in chromosome stability and are proposed to be biological determinants in the processes of tumorigenesis and aging (for reviews see Blackburn, 1991; Autexier and Greider, 1996; Greider, 1996; Blasco et al., 1997; Lee et al., 1998). Vertebrate telomeres consist of tandem repeats of the sequence TTAGGG (for review see Blackburn, 1991). In mammals, several TTAGGG repeat-binding proteins have been described that are essential for telomere function, such as TRF1, a negative regulator of telomere length (van Steensel and de Lange, 1997), and TRF2, which protects chromosome ends from fusions and it is involved in the formation of telomeric T-loops (van Steensel et al., 1998; Griffith et al., 1999). Telomeres are also binding sites for double strand break DNA repair proteins, such as Ku proteins and the Rad50–Mre11–Nsb1 complex that bind to TRF1 and TRF2, respectively (Bianchi and de Lange, 1999; Hsu et al., 1999; Zhu et al., 2000). Furthermore, a new member of the PARP family, named tankyrase (PARP-5; Smith et al., 1999), is located at human telomeres and is able to poly ADP-ribosylate itself as well as TRF1, inhibiting TRF1 binding to telomeric DNA and modulating telomere length (Smith and de Lange, 2000). Tankyrase has been proposed as a putative candidate to mediate DNA repair at the telomeres (Smith et al., 1999). The presence of DNA repair proteins at the telomeres suggest an interplay between telomeres and DNA repair pathways. On one hand, telomere length has been recently proposed to be one of the biological determinants of organismal sensitivity to ionizing radiation in man and mice (Goytisolo et al., 2000; Wong et al., 2000; McIlrath et al., 2001). Furthermore, mice and cells null for DNA repair proteins show telomeric phenotypes (Hsu et al., 2000; Samper et al., 2000; Goytisolo et al., 2001).

A previous report suggested that PARP-1 also had an essential role at the telomeres. In particular, mice deficient for PARP-1 activity (Wang et al., 1995) were found to have dramatically short telomeres, as well as numerous end-to-end fusions compared with wild-type controls (d'Adda di Fagagna et al., 1999). Here, we did a detailed telomere characterization of a different PARP-1$^{-/-}$ mouse (Menissier-de Murcia et al., 1997). Our results indicate that PARP-1$^{-/-}$ mice and PARP-1$^{-/-}$ primary cells show normal telomere length as determined by three independent techniques: quantitative telomeric (Q)-FISH, flow cytometry FISH (Flow-FISH), and telomere restriction fragment (TRF) analysis. The length of the G-strand overhang at the telomere was also normal in PARP-1$^{-/-}$ primary cells. Q-FISH and spectral karyotyping (SKY) analyses indicated that PARP-1$^{-/-}$ primary cells showed increased frequencies of chromosome breaks and fragments, as well as a slight increased in end-to-end fusions (Robertsonians and dicentrics) compared with wild-types. The frequency of end-to-end fusions detected in PARP-1$^{-/-}$ primary cells, however, was much lower than that described previously (d'Adda di Fagagna et al., 1999), 2 and 25 fusions per 100 metaphases, respectively. The end-to-end fusions that we detect in PARP-1$^{-/-}$ primary cells are likely to result from the DNA repair defect associated with PARP-1 deficiency (Trucco et al., 1998; Dantzer et al., 2000). It is important to note that both PARP-1$^{-/-}$ mice studied (d'Adda di Fagagna et al., 1999; this study) lacked PARP-1 activity, and did not show expression of any truncated forms of the PARP-1 protein (Trucco et al., 1998; for review see Bürkle et al., 2000). Furthermore, both PARP-1 knockout mice show similar phenotypes (Wang et al., 1995; Menissier-de Murcia et al., 1997; Beneke et al., 2000). Indeed, the absence of severe proliferative defects in these mice is more accordant with our finding of normal telomere function and a low frequency of end-to-end fusions. In summary, the results described here are in marked contrast to those described previously by d'Adda di Fagagna et al. (1999) and do not support a role for PARP-1 in regulating telomere length or in telomeric end-capping. We also show here that there is no direct interaction between PARP-1 and telomerase as indicated by the two-hybrid assay.

Results

Normal telomere length in PARP-1$^{-/-}$ mice and PARP-1$^{-/-}$ primary cells

We studied whether PARP-1 deficiency affects the length of TTAGGG repeats at the telomeres using PARP-1$^{-/-}$ mice (Menissier-de Murcia et al., 1997). For this, littermate wild-type, PARP-1$^{+/-}$, and PARP-1$^{-/-}$ mice or embryos derived from heterozygous crosses were used to quantify telomere length. Due to the fact that mouse telomeres show individual variability, it is essential to compare littermate mice, as well as to use several independent techniques to measure telomeres. Quantitative telomeric (Q)-FISH of wild-type, PARP-1$^{+/-}$ and PARP-1$^{-/-}$ littermate primary (passage 1) mouse embryonic fibroblasts (MEFs) revealed that all three genotypes showed a similar telomere length (Table I). The average telomere length was 35.24 ± 15.36, 40.29 ± 16.96, and 40.09 ± 15.85 Kb for wild-type (average of A10 and G4), PARP-1$^{+/-}$ (average of A7, E4, and G1), and PARP-1$^{-/-}$ (average of A6, E1, E2, G5, and G8) MEFs, respectively. These differences were not statistically significant (Student's t test, $P > 0.01$). It is noticeable that the standard deviations were also similar in the different genotypes, suggesting that telomeres were equally heterogeneous in length in all genotypes (see below). The Q-FISH data on MEFs was confirmed by using a different technique to measure telomere fluorescence based on Flow-FISH (described in Materials and methods; Table II). In this case, average telomere fluorescence expressed in arbitrary units was 3.51 ± 0.88, 3.69 ± 0.75, and 3.74 ± 0.67 for PARP-1$^{+/+}$ (average of A10 and G4), PARP-1$^{+/-}$ (average of A7, E4, and G1), and PARP-1$^{-/-}$ (average of A6, E1, E2, G5, and G8) MEFs, respectively. Again, these differences were not statistically significant (Student's t tests, $P > 0.01$). Histograms showing the frequency of a given telomere fluorescence in littermate wild-type (average of A10 and G4; a total of 3,972 telomeres), PARP-1$^{+/-}$ (average of A7, E4, and G1; a total of 5,500 telomeres), and PARP-1$^{-/-}$ (average of A6, E1, E2, G5, and G8; a total of 8,772 telomeres) MEFs are presented in Fig. 1. These histograms confirmed that the mean telomere fluorescence is similar in PARP-1$^{-/-}$, PARP-1$^{+/-}$, and wild-type MEFs, and furthermore showed that the heterogeneity of

Table I. **Chromosomal instability and telomere length determination by Q-FISH in PARP1$^{+/+}$, PARP1$^{+/-}$, and PARP1$^{-/-}$ littermate primary MEF cultures**

Genotype/litter[a]	Robertsonian translocations	Rings	Dicentrics	Fragments and breaks	Lacking telomeres	Telomere associations	Polyploid	Metaphases analyzed
PARP1$^{+/+}$A10	0	0	0	8	9	3	1	75
PARP1$^{+/-}$A7	1	0	1	11	23	8	3	75
PARP1$^{-/-}$A6	0	0	0	8	22	10	2	75
PARP1$^{+/-}$E4	0	1	1	12	9	12	2	75
PARP1$^{-/-}$E2	1	1	0	19	6	14	7	75
PARP1$^{-/-}$E1	0	0	0	13	23	16	10	75
PARP1$^{+/+}$G4	0	0	0	4	4	11	2	75
PARP1$^{+/-}$G1	1 clonal	0	0	15	6	20	4	75
PARP1$^{-/-}$G5	2	1	2	15 (3 minichr.)	5	14	7	75
PARP1$^{-/-}$G8	0	0	1	8	7	7	6	75
Totals								
All PARP1$^{+/+}$		0 (0%)[b]		12 (8%)	13 (8.6%)	14 (9.3%)	3 (2%)	150
All PARP1$^{+/-}$		5 (2.22%)		38 (16.8%)	38 (16%)	40 (17%)	9 (4%)	225
All PARP1$^{-/-}$		8 (2.13%)		63 (16.8%)	63 (16.8%)	61 (16.2%)	32 (8.5%)	375

Q-FISH Data

Litters	Genotype	Metaphases	q arm	p arm	Average p + q arms
A10	PARP1$^{+/+}$	15	41.48 ± 1934	31.37 ± 13.94	36.42 ± 16.64
A7	PARP1$^{+/-}$	15	50.17 ± 24.69	35.55 ± 13.72	42.86 ± 19.20
A6	PARP1$^{-/-}$	15	48.12 ± 22.92	38.39 ± 16.45	43.25 ± 19.62
E4	PARP1$^{+/-}$	10	45.51 ± 20.54	32.85 ± 14.88	39.18 ± 17.71
E2	PARP1$^{-/-}$	10	49.73 ± 23.32	34.95 ± 13.98	42.34 ± 18.65
E1	PARP1$^{-/-}$	10	39.54 ± 15.85	27.32 ± 11.03	33.43 ± 13.44
G4	PARP1$^{+/+}$	10	39.93 ± 17.33	28.15 ± 10.52	34.06 ± 14.01
G1	PARP1$^{+/-}$	10	46.31 ± 16.57	31.38 ± 11.36	38.84 ± 13.97
G5	PARP1$^{-/-}$	10	54.84 ± 20.65	43.20 ± 11.75	49.02 ± 16.2
G8	PARP1$^{-/-}$	10	38.67 ± 13.75	26.20 ± −8.86	32.43 ± 11.30

[a]Letters refer to the litter the MEFs were derived from.
[b]Percentage represents events per 100 metaphases.

telomeric lengths is similar in both genotypes, ruling out significant differences in telomere length between genotypes.

Flow-FISH on fresh splenocytes and bone marrow (BM) cells derived from wild-type, PARP-1$^{+/-}$, and PARP-1$^{-/-}$ littermate mice (8–12 wk old) also indicated that PARP-1$^{-/-}$ telomeres were similar in length to those of heterozygous and wild-type littermates (Table III). In the case of fresh splenocytes, the average telomere fluorescence values were 2.92 ± 0.66, 2.93 ± 0.47, and 2.68 ± 0.91 for wild-type (average of mice V32, V36, V64, V66, V74, V97, and V110), PARP-1$^{+/-}$ (average of mice V35, V37, V67, V100, and V107), and PARP-1$^{-/-}$ (average of V29, V30, V33, V65, V69, V75, V98, V99, V106, and V109). Similarly, Flow-FISH on fresh bone marrow cells indicated average telomere fluorescence values of 3.34 ± 0.49, 2.92 ± 0.77, and 3.30 ± 0.50 for wild-type (average of mice V32, V36, V64, V66, V74, V97, and V110), PARP-1$^{+/-}$ (average of mice V35, V37, V67, V100, and V107), and PARP-1$^{-/-}$ (average of V29, V30, V33, V65, V69, V75, V98, V99, V106, and V109). Again the differences in average telomere length between genotypes were not statistically significant ($P > 0.01$). These results are in agreement with the Q- and Flow-FISH data on MEFs and were obtained with five independent litters derived from heterozygous crosses (Table III).

Finally, telomere length was also evaluated by Southern blot as an alternative technique to measure telomere length not based on fluorescence. Primary BM cells or splenocytes, as indicated, from four wild-type (V64, V66, V74, and V110), two PARP-1$^{+/-}$ (V67 and V107), and five PARP-1$^{-/-}$ (V65, V69, V75, V106, and V109) littermate mice were subjected to TRF analysis as described (Materials and methods; Fig. 2). TRF analysis also showed a similar telomere length in primary (passage 1) MEFs from littermate wild-type (D9) and PARP-1$^{-/-}$ (D7 and D11) embryos (Fig. 2).

Together, these data strongly indicate that PARP-1 deficiency in mice or in primary cells does not result in significant telomere length alterations.

Chromosomal instability in PARP-1$^{-/-}$ cells: Q-FISH and SKY analyses

To study the impact of PARP-1 deficiency on telomere function, we analyzed the involvement of telomeres in the chromosomal aberrations spontaneously arising in true primary (passage 1) PARP-1$^{-/-}$ MEFs. For this, we performed Q-FISH of metaphasic nuclei with a fluorescent PNA-telomeric probe (Zijlmans et al., 1997) and then we scored for chromosomal aberrations (see "Q-FISH" in Materials and methods for description of different aberrations). Spontaneously arising chromosome aberrations were analyzed on at least 75 metaphases of each one of the primary (passage 1) wild-type, PARP-1$^{+/-}$, and PARP-1$^{-/-}$ MEF cultures derived from heterozygous crosses (a total of 150, 225, and 375 metaphases for each genotype, respectively). As displayed in Table I, an increase in the frequency of chromosome/chromatid breaks and fragments was detected in primary MEFs isolated from PARP-1$^{-/-}$ or PARP-1$^{+/-}$ when compared with wild-type controls, 16.8,

Table II. **Measurement by Flow-FISH of telomere length in embryonic fibroblasts obtained from PARP$^{+/-}$ heterozygote crosses**

Embryos	Litter	Genotype	Telomere length[a]
A6	1	−/−	3.08
A7		+/−	2.91
A10		+/+	2.89
E1	2	−/−	3.07
E2		−/−	4.36
E3		−/−	4.02
E4		+/−	4.42
G1	3	+/−	3.76
G4		+/+	4.14
G5		−/−	4.61
G8		−/−	3.34

[a]Telomere length is expressed in arbitrary fluorescence units which have been normalized against a calibration curve on R and S cells (see Materials and methods).

16.8, and 8 events per 100 metaphases, respectively (Table I and Fig. 3 A). Primary MEFs isolated from PARP-1$^{-/-}$ or PARP-1$^{+/-}$ also showed a small increase in end-to-end fusions (Robertsonians+dicentrics+chromosome rings) compared with wild-type controls, 2.13, 2.22, and 0 fusions per 100 metaphases, respectively (Table I and Fig. 3 A). In some PARP-1$^{-/-}$ metaphases where Robertsonian-like fusions were detected, we were able to find the telomeric fragments resulting from the Robertsonian translocation (Fig. 3 C). These fragments always showed normal telomeres (Fig. 3 C), indicating that these fusions were the result of true Robertsonian translocations and not the consequence of telomere shortening. These Robertsonian fusions are different from those found in late generation telomerase-deficient mice that have critically short telomeres (Blasco et al., 1997). Furthermore, the fact that fusions detected in PARP-1$^{-/-}$ primary cells did not contain telomeres at the fusion point indicates that they are also different from those described in cells with impaired TRF2 function (van Steensel et al., 1998) or in cells deficient for nonhomologous end-joining DNA repair proteins such as Ku86 and DNA-PKc's (Bailey et al., 1999; Hsu et al., 2000; Samper et al., 2000; Goytisolo et al., 2001), all of which showed long telomeres at the fusion point (see Discussion).

A slightly increased frequency of telomeric associations (two chromosomes which are associated, not fused, by their telomeres; four telomeric dots should be present at the association point) was also found in MEFs isolated from PARP-1$^{-/-}$ or PARP-1$^{+/-}$ as compared with wild-type controls, 16, 17, and 9.3 telomeric associations per 100 metaphases, respectively (Table I). Primary PARP-1$^{-/-}$ MEFs also showed an increased frequency of polyploidies, 8.5, 4, and 2%, for PARP-1$^{-/-}$, PARP-1$^{+/-}$, and PARP-1$^{+/+}$, respectively (Table I). A higher frequency of chromosome ends lacking detectable TTAGGG was also found in the PARP-1$^{-/-}$ and PARP-1$^{+/-}$ MEF, as compared with wild-type controls, 16.8, 16, and 8.6%, respectively. This increased frequency of ends lacking detectable TTAGGG repeats cannot be attributed to telomere shortening, as telomere length is normal in PARP-1 mice (see above), and it is likely to be the consequence of the increased frequencies of chromosome/chromatid breaks in these cells (see above).

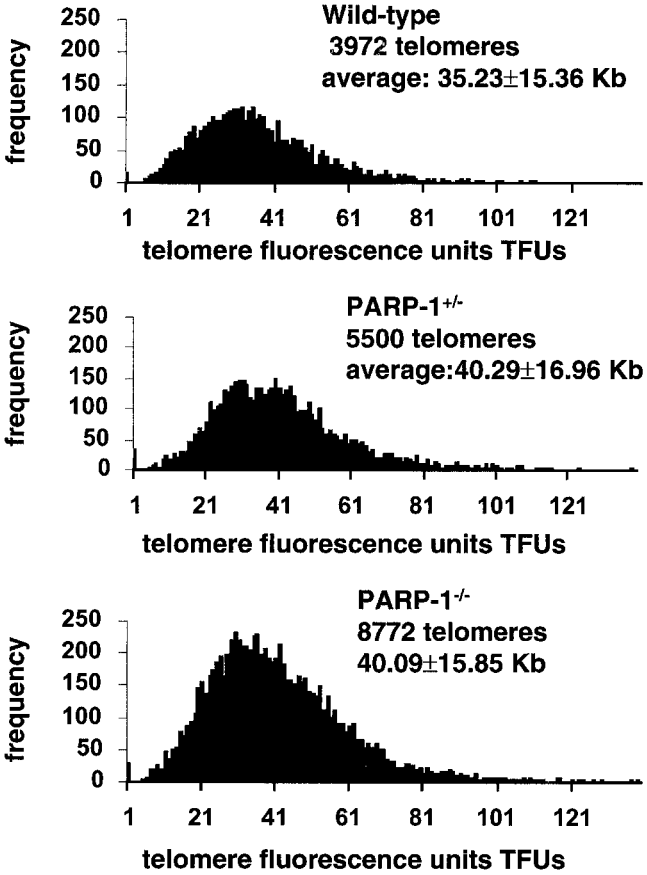

Figure 1. **Telomere fluorescence distribution in wild-type, PARP-1$^{+/-}$, and PARP-1$^{-/-}$ MEFs.** Telomere length distribution in several different littermate wild-type (A10 and G4), PARP-1$^{+/-}$ (A7, E4, and G1), and PARP-1$^{-/-}$ (A6, E1, E2, G5, and G8) primary MEFs. The histogram depicts similar telomeres in all genotypes. One TFU corresponds to 1 Kb of TTAGGG repeats (see Table I and Table II for telomere length values in MEFs).

Chromosome fusions are associated with the occurrence of anaphase bridges during mitosis due to a failure to separate sister chromatids (McClintock, 1941, 1942; for review see de Lange, 1995). In agreement with this, we found that PARP-1$^{-/-}$ primary MEFs showed a significantly increased frequency of anaphase bridges compared with control cells. The frequencies of anaphase bridges were 0.833 and 0.105 per anaphase for wild-type and PARP-1$^{-/-}$ MEFs, respectively (Fig. 3 B). This difference is significant, as indicated by a Student's t test value $P = 0.0042$. A similar frequency of anaphase bridges has been described recently for DNA-PKcs$^{-/-}$ primary MEFs, which have a similar frequency of end-to-end fusions to that described here for primary PARP-1$^{-/-}$ cells (Goytisolo et al., 2001).

It is important to note that the frequency of spontaneous chromosome/chromatid breaks and fragments that we found in primary PARP-1$^{-/-}$ MEFs (16.8%) is similar to that described previously, which was 10% (d'Adda di Fagagna et al., 1999). Strikingly, the frequency of end-to-end fusions that we find in primary PARP-1$^{-/-}$ cells is dramatically lower than that described previously (d'Adda di Fagagna et al., 1999), 2.13 and 25.0 fusions per 100 metaphases, respectively (see Discussion). Interestingly, PARP-1$^{-/-}$ cells that

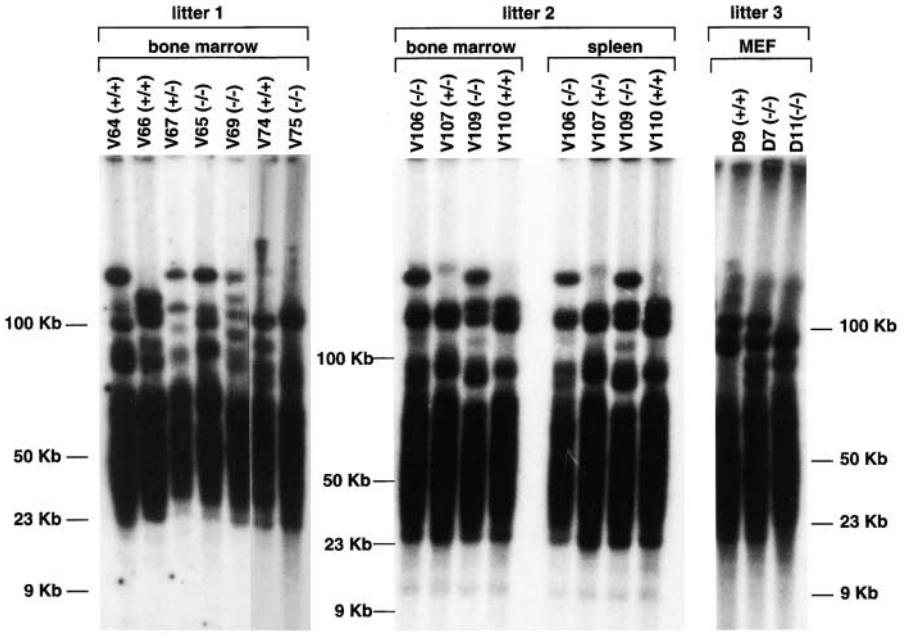

Figure 2. **TRF analysis in wild-type, PARP-1$^{+/-}$, and PARP-1$^{-/-}$ primary cells.** TRF analysis of primary BM cells or splenocytes, as indicated, from four wild-type (V110, V64, V66, and V74), two PARP-1$^{+/-}$ (V107 and V67), and five PARP-1$^{-/-}$ (V106, V109, V65, V69, and V 75) littermate mice. TRF analysis of primary (passage 1) MEFs from littermate wild-type (D9) and PARP-1$^{-/-}$ (D7 and D11) embryos is also shown. Notice that TRF signals are similar in size in PARP-1$^{-/-}$, PARP-1$^{+/-}$, and wild-type.

were kept in culture for 26 population doublings showed an increased frequency of end-to-end fusions compared with the primary cultures (Table IV). This increased frequency of end-to-end fusions was closer to that described by d'Adda di Fagagna et al. (1999). Hence, the increased end-to-end fusions in cultured PARP-1$^{-/-}$ cells could explain the different outcomes between both studies (see Discussion).

Table III. **Measurement by Flow-FISH of telomere length in splenocytes and bone marrow cells obtained from +/+, +/−, and −/− PARP-1 littermate mice of different litters**

Mice	Litter	Genotype	Spleen	Bone marrow
			Telomere length[a]	Telomere length
V29 (M)	1	−/−	1.74	2.88
V30 (M)		−/−	1.79	2.71
V32 (M)		+/+	2.44	2.82
V33 (F)		−/−	1.17	3.56
V35 (F)		+/−	2.76	3.01
V36 (F)		+/+	2.36	3.02
V37 (F)		+/−	2.84	2.13
V64 (M)	2	+/+	3.16	3.22
V65 (M)		−/−	3.15	3.52
V66 (M)		+/+	3.37	3.54
V67 (M)		+/−	3.28	3.62
V69 (F)		−/−	3.22	3.34
V74 (M)	3	+/+	3.82	4.32
V75 (M)		−/−	3.91	4.19
V97 (F)	4	+/+	3.36	3.44
V98 (F)		−/−	3.86	3.79
V99 (F)		−/−	2.70	3.45
V100 (F)		+/−	3.52	3.73
V106 (F)	5	−/−	2.85	2.92
V107 (F)		+/−	2.29	2.13
V109 (F)		−/−	2.44	2.64
V110 (F)		+/+	1.99	3.05

[a]Telomere length is expressed in arbitrary fluorescence units which have been normalized against a calibration curve on R and S cells (see Materials and methods). F, female; M, male.

As an independent technique to study chromosomal aberrations, SKY analysis of the PARP-1$^{-/-}$ primary MEFs revealed similar frequencies of end-to-end fusions and breaks than Q-FISH (2 end-to-end fusions per 100 metaphases), and it allowed us to identify which chromosomes were involved in such rearrangements. End-to-end fusions and telomeric associations always involved nonhomologous chromosomes as determined by SKY (Fig. 3, D and E), further supporting the evidence that they were true Robertsonian translocations and not the consequence of telomere shortening. Breaks were also mapped by SKY and they seemed to occur randomly through all chromosome lengths, since a significant recurrent breakpoint was not noted (Fig. 3 E).

Normal length telomeric G-strand overhangs in PARP-1$^{-/-}$ cells

G-strand overhangs are regions of G-rich single-stranded telomeric DNA that protrude in the 3′ direction from the double-stranded telomere. These single-stranded G-rich regions have been involved recently in the formation of a special structure at the chromosome end named T-loop, which has been proposed to protect the ends from recombination and DNA repair activities (Griffith et al., 1999). Hence, examination of telomeric G-strand overhangs in PARP-1 null cells is crucial to gain more insight into the telomere integrity of these cells. To study the telomeric G-strand overhangs, we carried out TRF analysis with a $(CCCTAA)_4$ probe as described (Samper et al., 2000) using nondenaturing pulse field agarose gels (Materials and methods). Detection of a signal with the $(CCCTAA)_4$ probe hybridized to native DNA samples indicates the presence of the G-strand overhang. Primary wild-type and PARP-1$^{-/-}$ MEFs showed G-strand–specific signals that were similar in size and intensity in all genotypes (Fig. 4). Table V shows quantification of the G-strand signals; the wild-type values were normalized to 100 in each litter. The average G-strand signal for

Table IV. **Chromosomal instability using Q-FISH on PARP-1$^{+/+}$ and PARP-1$^{-/-}$ MEF cultures passaged for 26 population doublings (PD26)**

Genotype	Robertsonian translocations	Rings	Dicentrics	Fragments and breaks	Minichrom.	Telomere associations	Polyploid	Metaphases analyzed
PARP1-1$^{+/+}$ (PD26)	0	0	0	8	5	16	24	26
PARP1-1$^{+/+}$ (PD26)	0	0	0	4	2	27	22	29
PARP1-1$^{-/-}$ (PD26)	0	0	4	11	2	26	12	21
PARP1-1$^{-/-}$ (PD26)	0	1	1	11	33	20	29	29
Totals								
All PARP1-1$^{+/+}$		0 (0%)[a]		12 (21%)	7 (12%)	43 (78%)	46 (83%)	55
All PARP1-1$^{-/-}$		6 (12%)		22 (44%)	35 (70%)	46 (92%)	41 (82%)	50

Notice that at PD26 most of the PARP-1$^{+/+}$ and PARP-1$^{-/-}$ MEF cultures were polyploid. PARP-1$^{-/-}$ cells showed a higher frequency of end-to-end fusions (RIC+R+DIC) than the similarly passaged wild-type cultures and the primary (PD2) PARP-1$^{-/-}$ cells (see Fig. 1): 12 and 2 end-to-end fusions per 100 metaphases, respectively. The frequencies of breaks and fragments and that of minichromosomes were also increased in passaged PARP-1$^{-/-}$ cells compared to wild-type controls. The frequency of telomeric associations in passaged wild-type and PARP-1$^{-/-}$ cells was similar, in agreement with a normal telomere end-capping function in these cells.
[a]Percentage represents events per 100 metaphases.

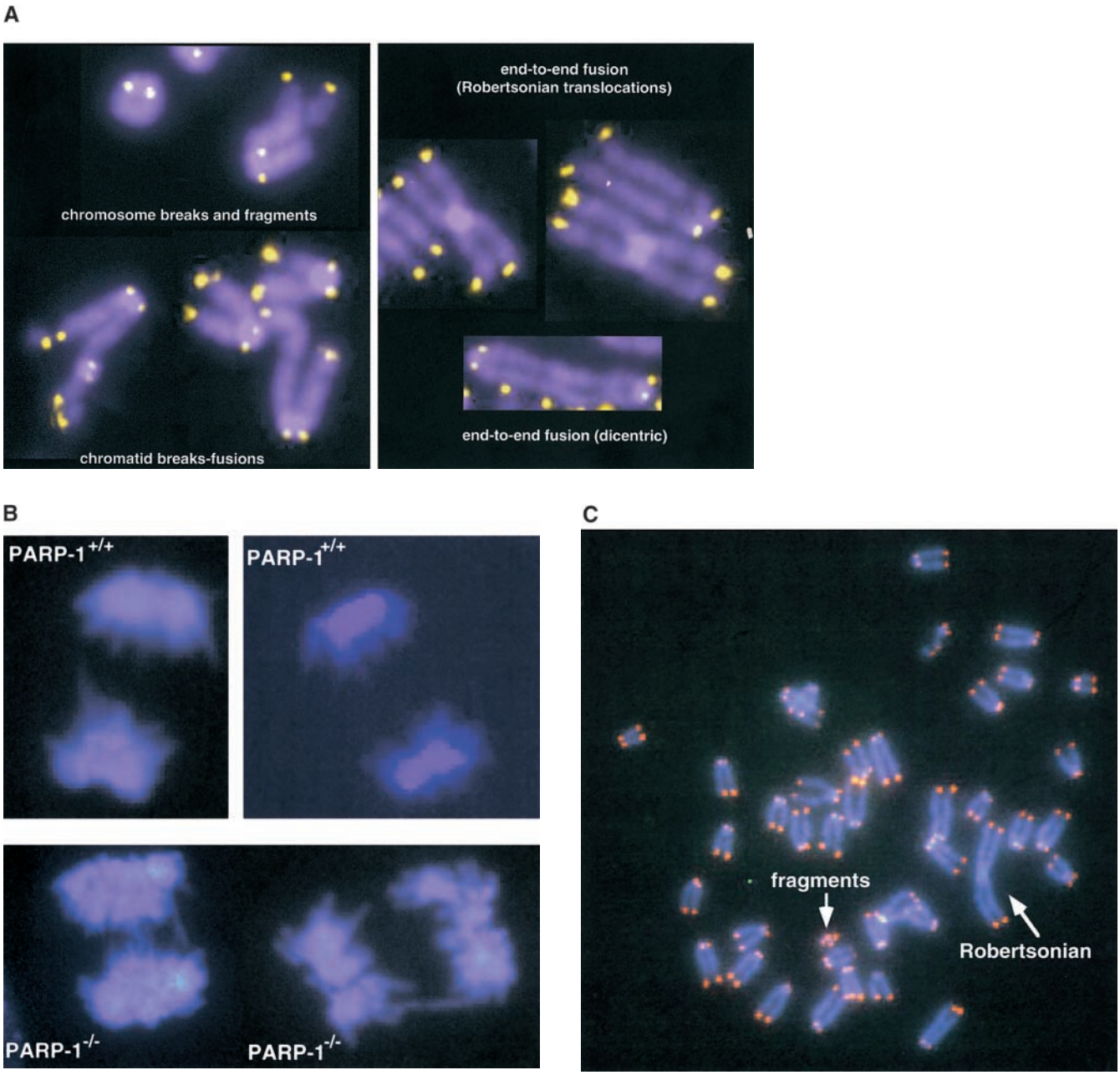

Figure 3 (continues on facing page)

PARP-1$^{-/-}$ MEFs was 120% that of the wild-types; however, this difference was not statistically significant (Student's t test, $P = 0.24$). To show that the probe specifically recognized the single-stranded telomeric tail, treatment with mung bean nuclease that specifically degrades single-stranded DNA and RNA overhangs was performed. As expected, the G-strand signal decreased in all genotypes upon treatment, as shown in Fig. 4 ("native gel"). As control, the same gel was denatured and rehybridized with the $(CCCTAA)_4$ probe, which highlighted the TRFs (Fig. 4; "denaturing gel"), again showing no difference in TRF lengths between wild-type and PARP-1$^{-/-}$ genotypes.

Collectively, these results show that PARP-1 deficiency in mammals does not result in loss or significant deregulation of the G-strand overhang length.

Telomerase reverse transcriptase is not a direct target of PARP-1

A direct interaction between PARP-1 and DNA polymerase α-primase tetramer has been demonstrated through the catalytic subunit of DNA polymerase α and the PARP-1 DNA binding domain, suggesting a link between DNA strand break detection and DNA replication (Simbulan-Rosenthal et al., 1996; Dantzer et al., 1998). Since telomerase is the cellular reverse transcriptase involved in replicating telomeric DNA (for review see Nugent and Lundblad, 1998), we investigated whether the catalytic subunit of telomerase, Tert, could also interact or be a target of PARP-1 activity. For this, we first determined telomerase activity levels in wild-type and in PARP-1$^{-/-}$ cells which lack PARP-1 activity. As shown in Fig. 5, telomerase activity levels are similar

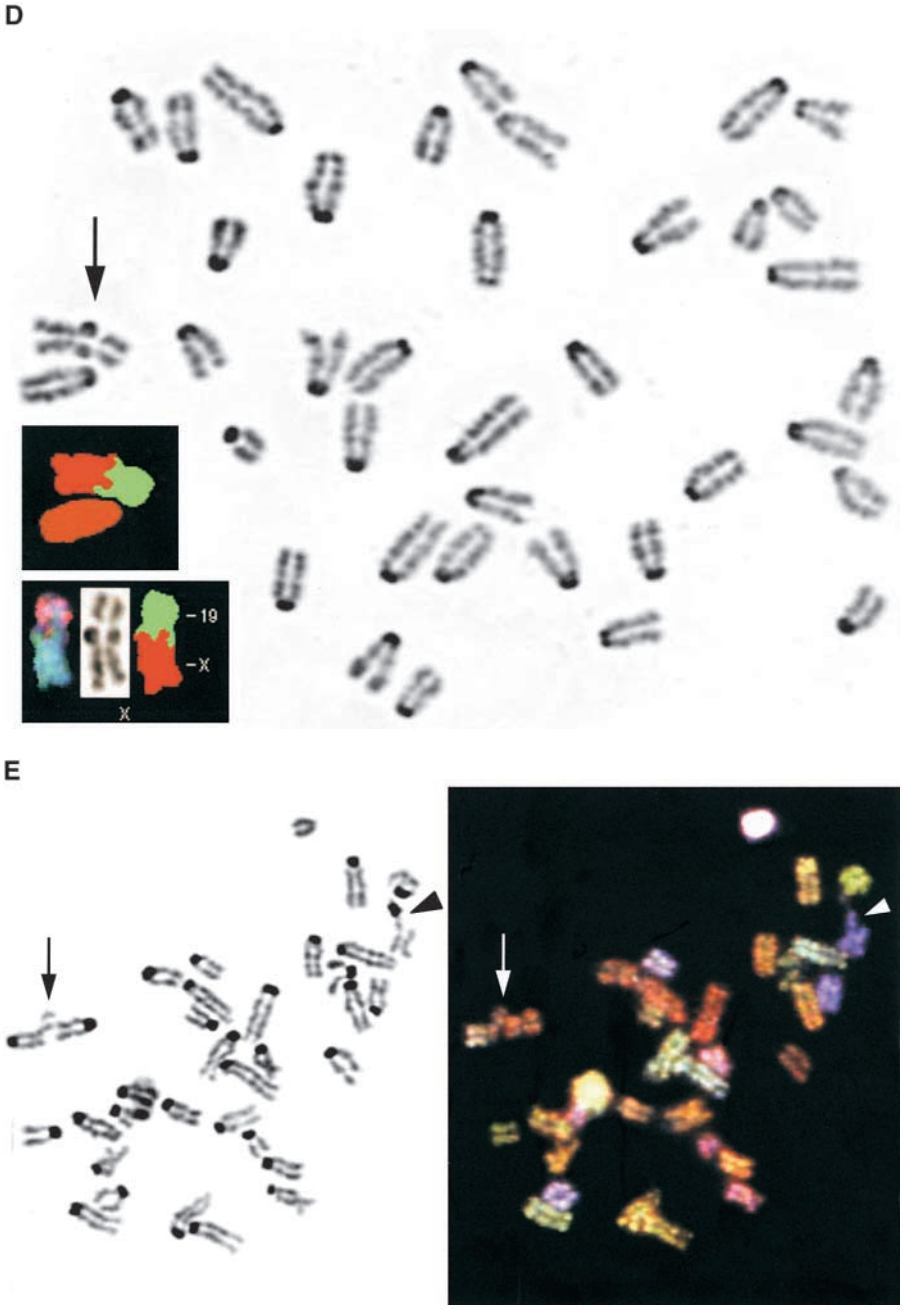

Figure 3. **Chromosomal instability in wild-type, PARP-1$^{+/-}$, and PARP-1$^{-/-}$ MEFs.** (A) Cytogenetic alterations detected in PARP-1$^{-/-}$ metaphases from primary MEFs after hybridization with DAPI and a fluorescent Cy-3–labeled PNA-telomeric probe. For quantifications see Table I. Blue color corresponds to chromosome DNA stained with DAPI; yellow and white dots correspond to TTAGGG repeats. For definition of the different aberrations see Materials and methods. The different kinds of aberrations detected are indicated in the Figure. (B) Representative images of anaphase bridges in PARP-1$^{-/-}$ cells. Blue color corresponds to chromosome DNA stained with DAPI. (C) Representative image of a metaphase showing a typical Robertsonian translocation and the corresponding fragment with normal telomeres (indicated by arrows). (D) A metaphase spread showing a chromosome fusion in PARP-1$^{-/-}$ primary MEFs (indicated with an arrow). SKY detected that the fusion involves chromosomes X and 19. SKY analysis is shown as two insets: the top inset shows the same chromosome fusion after color classification, and the bottom inset shows the karyotype-arranged chromosomes with the direct fluorochrome image (left), DAPI counterstain (middle), and classified chromosomes (right). (E) A metaphase spread of PARP-1$^{-/-}$ MEFs showing the DAPI staining (left) and the SKY spectral image (right). The arrow indicates an association between chromosomes 6 and 10. A break was also present in the same rearrangement (the arrowhead points to a single break affecting chromosome 7).

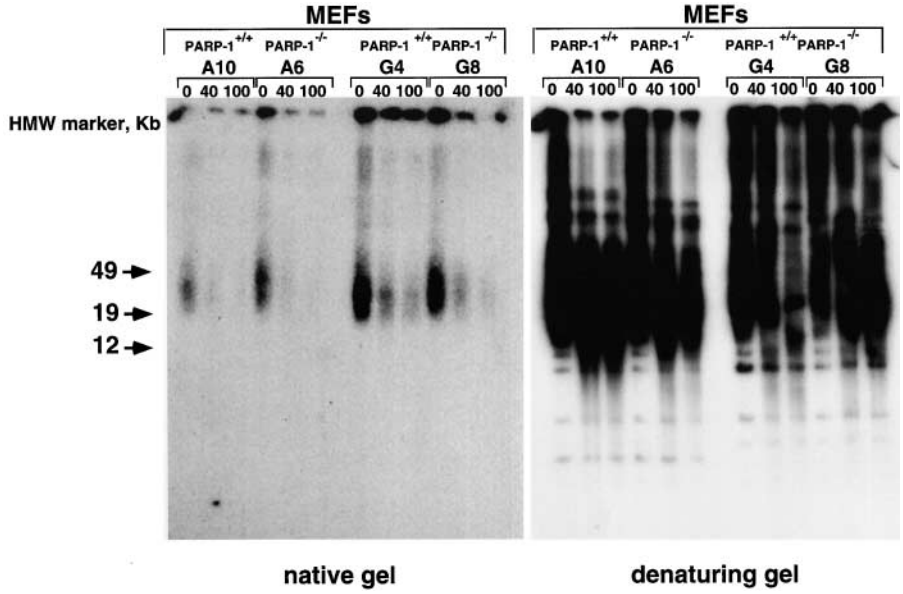

Figure 4. **Normal G-strand overhang in PARP-1$^{-/-}$ primary cells.** G-strand overhangs in littermate wild-type and PARP-1$^{-/-}$ MEFs are visualized in native gel after hybridization with a $(CCCTAA)_4$ probe (see Materials and methods). Notice that upon treatment with two different doses of mung bean nuclease (40 and 100 U) the G-strand–specific signal decreases. As control, the same gel was denatured and reprobed with the $(CCCTAA)_4$ probe to visualize telomeres. A10 and A6 are littermate wild-type and PARP-1$^{-/-}$ MEFs, respectively. G4 and G8 are littermate primary MEF cultures.

in wild-type (A10 and G1), PARP-1$^{+/-}$ (A7), and PARP$^{-/-}$ (A6, G8, and E1) primary MEF cultures, indicating that lack of PARP-1 activity does not significantly affect the levels of telomerase activity in the cell. A similar absence of changes in telomerase activity between wild-type and PARP-1$^{-/-}$ cells was obtained upon treatment of cells with genotoxic agents such as gamma irradiation and H_2O_2 which dramatically activate PARP-1 (not shown).

These data suggest that PARP-1 activity does not regulate telomerase activity. However, PARP-1 might be able to interact directly with Tert. To address this, we carried out two-hybrid assays (see Materials and methods). As control for the two-hybrid assay we show interaction between the cell cycle proteins CDK4 and p16 as described previously (Table VI; Serrano et al., 1993). No interaction was detected between PARP-1 and mTert in the two-hybrid assay (Table VI).

Together, these results suggest that (a) PARP-1 activity does not modulate telomerase activity in primary MEFs, and (b) that there is no direct interaction between PARP-1 and the catalytic subunit of telomerase, Tert.

Discussion

Increasing evidence from yeast and mammals suggests that DNA double strand break repair proteins have a role at the telomeres besides their role in DNA repair (Boulton and Jackson, 1996; Bailey et al., 1999; Nugent et al., 1998; Martin et al., 1999; Mills et al., 1999; Hsu et al., 2000; Samper et al., 2000; Goytisolo et al., 2001). In mammals, components of the DNA–PK (Ku70–Ku86–DNA-PKc's) and the Rad50–Mre11–NSB1 DNA repair complexes have been proposed to bind and protect telomeres from fusions (Bianchi et al., 1999; Hsu et al., 1999, 2000; Samper et al., 2000; Zhu et al., 2000; Goytisolo et al., 2001). In particular, mice deficient for Ku86 or DNA-PKc's show increased frequencies of telomere fusions (Bailey et al., 1999; Hsu et al., 2000; Samper et al., 2000; Goytisolo et al., 2001), and the Rad50–Mre11–NSB1 complex has been shown to interact with the telomeric protein TRF2 (Zhu et al., 2000).

Several studies have shown an interaction between the ADP-ribosylating enzyme PARP-1 and the DNA repair proteins DNA-PKc's and Ku (Morrison et al., 1997; Ruscetti et al., 1998; Ariumi et al., 1999; Galande and Kohwi-Shigematsu, 1999). Furthermore, a novel ADP-ribosylating enzyme named tankyrase, or PARP-5, has been found at telomeres and has a role in regulating telomere length in mammals through its interaction with TRF1, linking ADP-ribosylation with telomere function (Smith et al., 1999; Smith and de Lange, 2000). The generation of several knockout mice for PARP-1 allows us to evaluate the putative

Table V. **Quantification of G-strand overhang signal in wild-type and PARP-1$^{-/-}$ MEFs**

Mice[a]	Litter	Genotype	Signal[b]	Percentage[c]
A10	1	+/+	31,995	100
A6		−/−	35,681	111.5
G4	2	+/+	56,945	100
G8		−/−	72,809	127.9

[a]These samples were MEFs.
[b]The intensity of the signal is expressed in arbitrary units.
[c]The percentage is expressed in relation to the wild-type littermate.

Table VI. **PARP does not interact with mTERT in a two-hybrid assay**

Plasmids transfected			
pGBT	pGAD	Medium	Colonies
Empty	−	−Trip	+++
−	Empty	−Leu	+++
mTERT	−	−Trip	+++
−	PARP	−Leu	++
CDK4	−	−Trip	++
−	p16	−Leu	++
Empty	Empty	−Trip, Leu, His	−
mTERT	Empty	−Trip, Leu, His	−
Empty	PARP	−Trip, Leu, his	−
mTERT	PARP	−Trip, Leu, His	−
CDK4	p16	−Trip, Leu, His	++

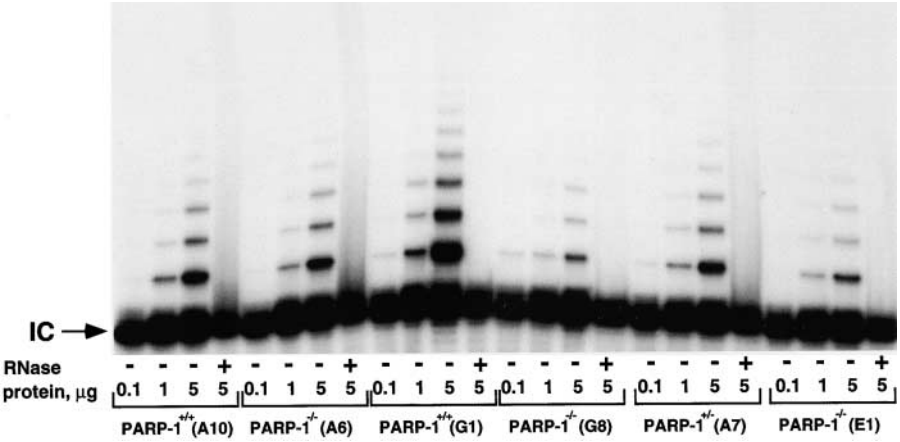

Figure 5. **Telomerase activity in wild-type, PARP-1$^{+/-}$, and PARP-1$^{-/-}$ MEFs.** S-100 extracts were prepared from wild-type (A10 and G1), PARP-1$^{+/-}$ (A7), and PARP$^{-/-}$ (A6, G8, and E1) primary MEFs cultures and assayed for telomerase activity. Extracts were pretreated (+) or not (−) with RNase. Protein concentration used is indicated. The arrow indicates the internal control (IC) for PCR efficiency. Same letter refers to littermate embryos.

role of PARP-1 activity at the mammalian telomere. In particular, exon 1 (Matsutani et al., 1999), exon 2 (Wang et al., 1995), and exon 4 (Menissier-de Murcia et al., 1997) of the PARP-1 gene have been interrupted by homologous recombination. In all cases, the knockout mice lacked PARP-1 activity, and did not show expression of any truncated forms of the PARP-1 protein (Trucco et al., 1998; for review see Bürkle et al., 2000). Furthermore, all three different PARP-1$^{-/-}$ mice showed similar phenotypes (Wang et al., 1995; Menissier-de Murcia et al., 1997; Matsutani et al., 1999; Beneke et al., 2000). A previous study reported that the PARP-1–deficient mice generated by Wang et al. (1995) had dramatically shortened telomeres and a very high chromosomal instability, consisting mostly of end-to-end fusions (up to 25 end-to-end fusions per 100 metaphases; d'Adda di Fagagna et al., 1999). These results suggested that PARP-1 was one of the major players in regulating telomere length and telomeric end-capping function. In marked contrast to that, and using a panoply of assays to measure telomere length such as Q-FISH, Flow-FISH, and TRF analysis, we found no significant alterations in telomere length in the PARP-1$^{-/-}$ mice and PARP-1$^{-/-}$ primary cells studied here. As mentioned above, both PARP-1$^{-/-}$ mouse models lack PARP-1 activity and show similar phenotypes (Wang et al., 1995; Menissier-de Murcia et al., 1997; Beneke et al., 2000). The differences in telomere length between both studies cannot be attributed to transdominant effects of putative truncated forms of PARP-1 in any of these two knockout models, since there is no evidence that either PARP-1$^{-/-}$ model express such truncated PARP-1 proteins when using a wide range of antibodies (Trucco et al., 1998; see below).

Importantly, telomere length was not the only apparent difference between the current study and that published previously by d'Adda di Fagagna et al. (1999). In our study, both Q-FISH and SKY analyses indicated that PARP-1$^{-/-}$ primary cells have increased frequencies of chromosome/chromatid breaks and fragments, as well as a low frequency of end-to-end fusions of 2 fusions per 100 metaphases (Robertsonian-like fusions, dicentrics, and rings). Although the frequency of chromosome/chromatid breaks and fragments that we found was similar to that described in d'Adda di Fagnana et al. (1999), the frequencies of end-to-end fusions were 2 and 25 end-to-end fusions per 100 metaphases in this study and that of d'Adda di Fagnana et al. (1999), respectively. The low frequency of end-to-end fusions detected here in PARP-1$^{-/-}$ primary cells can be fully explained by the fact that PARP-1 deficiency results in a defective DNA repair (D'Amours et al., 1999; for review see Bürkle et al., 2000; Shall and de Murcia, 2000) without invoking a telomere dysfunction. Furthermore, the frequency of end-to-end fusions that we detect in PARP-1$^{-/-}$ primary cells (2 fusions in 100 metaphases) is more accordant with the fact that all PARP-1 knockout models are fertile and viable and do not show any of the extreme phenotypes (i.e., severe proliferative defects, premature aging, infertility) shown by late generation telomerase knockouts or Ku86 knockouts (Herrera et al., 1999; Samper et al., 2000), which have a frequency of end-to-end fusions similar to that published by d'Adda di Fagagna et al. (1999) for PARP-1$^{-/-}$ mice. In summary, the extensive data presented here does not support the previous notion that PARP-1 activity has an essential role in regulating telomere length or telomeric end-capping function (d'Adda di Fagagna et al., 1999), and other factors might have masked this conclusion in the previous study by d'Adda di Fagagna et al. (1999). A possible explanation for the different outcomes of both studies could be that we used true primary cells (population doubling two at the most). It is known that cells deficient for genes that are important in chromosomal stability accumulate greater numbers of chromosomal aberrations as they are passaged in culture (i.e., telomerase-deficient cells; Hande et al., 1999). In this regard, we have observed significantly increased frequencies of end-to-end fusions in PARP-1$^{-/-}$ cells that have been kept in culture for 26 population doublings as compared with similarly passaged wild-type cells or to primary PARP-1$^{-/-}$ cells. Hence, using cells which are not strictly primary cells could explain some of the differences between both studies.

Finally, we have not found differences in telomerase activity between PARP-1$^{-/-}$ cells and the corresponding wild-type cells, suggesting that PARP-1 activity does not regulate telomerase activity; this observation agrees with that reported previously by d'Adda di Fagagna et al. (1999). In addition, we have been able to show here that there is no direct interaction between PARP-1 and Tert, the telomerase catalytic subunit, using the two-hybrid assay. Since PARP-1 has been located at the replication complex, our results suggest that PARP-1 does not interact directly with Tert when telomerase is active replicating telomere ends.

Materials and methods

Mice and cells

PARP-1$^{-/-}$ mice were described elsewhere (Menissier-de Murcia et al., 1997). Wild-type, PARP-1$^{+/-}$, and PARP-1$^{-/-}$ mice or cells were derived from heterozygous crosses and, for all studies, littermate mice or primary cells (passage 1) were used. Mice used for Q-FISH and Flow-FISH studies ranged between 8 to 12 wk old. MEFs were prepared from day 13.5 embryos derived from heterozygous crosses as described (Blasco et al., 1997). First passage MEFs used in the different experiments corresponded to ~2 population doublings.

Mice handling

All mice were housed at our barrier area in Madrid, where pathogen-free procedures are used in all mouse rooms. Quarterly health monitoring reports have been negative for all pathogens in accordance with FELASA recommendations (Federation of European Laboratory Animal Science Associations).

Scoring of chromosomal abnormalities by telomere Q-FISH and SKY

Telomere Q-FISH. 75 metaphases of each culture of wild-type, PARP-1$^{+/-}$, and PARP-1$^{-/-}$ MEFs (a total of 150, 225, and 375 for each genotype, respectively) were scored for telomere fusions, chromatid breaks, and chromosome fragments by superimposing the telomere image on the DAPI chromosome image in the TFL-telo software (gift from Dr. Peter Lansdorp, Terry Fox Laboratory, B.C. Cancer Research Center, Vancouver, British Columbia, Canada). The following criteria were applied: end-to-end fusions, chromosomes fused by their ends (end-to-end fusions can be two chromosomes fused by their p arms [Robertsonian-like fusions] or two chromosomes fused by their q arms [dicentrics]; telomere associations, chromosomes with four distinct telomere signals but aligned less than 1/2 chromatid apart; breaks, gaps in a chromatid whose corresponding chromosome was identified; chromosome fragments, chromosome pieces (with two telomeres or less) whose corresponding chromosome was not easily identified.

To score for anaphase bridges, primary MEF cultures were seeded on microscope slides and stained with DAPI to visualize the DNA. At least twenty anaphases were scored for each wild-type and PARP-1$^{-/-}$ culture and the anaphase bridges counted.

SKY. Painting probes for each chromosome were generated from flow-sorted mouse chromosomes using sequence-independent DNA amplification. Labeling was performed by directly incorporating four different dyes in a combination sequence that allows unique and differential identification of each chromosome. Slides were prepared from the fixative-stored material and were hybridized using the SKY method according to the manufacturer protocol (Applied Spectral Imaging). In brief, hybridization was performed for 2 d at 37°C. Washing and detection of fluorochromes was done as instructed by the manufacturer. Chromosomes were counterstained with DAPI. Images were acquired with spectracube (C-4880; Applied Spectral Imaging) mounted on a microscope (Axioplan; ZEISS) using a custom designed optical filter, SKY-1 (Chroma Technology). Placing an Sagnac interferometer (Applied Spectral Imaging) in the optical head, an interferogram was generated at all image points, which was deduced from the optical path difference of the light which, in turn, depended on the wave length of the emitted fluorescence. The spectrum was recovered by Fourier transformation, and the spectral information was displayed by assigning red (R), green (G), or blue (B) colors to certain ranges. This RGB display rendered chromosomes that were labeled with spectrally overlapping fluorochromes or fluorochrome combinations in similar colors. Based on the measurement of the spectrum for each chromosome, a spectral classification algorithm was applied that allowed the assignment of a pseudocolor to all points in the image that have the same spectrum. This algorithm formed the basis for chromosome identification by SKY. As a result of this process, three different images are produced for each image (or metaphase). The black and white DAPI, the RGB-based, and the classified images offered a complete approach of each metaphase and allowed the specific and simultaneous identification of each chromosome pair.

50 additional metaphases of each culture of wild-type and PARP-1$^{-/-}$ MEFs were captured and analyzed by SKY, and chromosomal abnormalities were scored as above.

Statistical analysis

Statistical calculation was done using Microsoft Excel. For statistical significance, Student's *t* test values were calculated.

Telomere length analysis

Q-FISH. First passage MEFs were prepared for Q-FISH as described (Samper et al., 2000). Q-FISH hybridization was carried out as described (Samper et al., 2000). To correct for lamp intensity and alignment, images from fluorescent beads (Molecular Probes) were analyzed using the TFL-Telo program. Telomere fluorescence values were extrapolated from the telomere fluorescence of LY-R (R cells) and LY-S (S cells) lymphoma cell lines (Alexander and Mikulski, 1961) of known lengths of 80 and 10 Kb (McIlrath et al., 2001). There was a linear correlation ($r^2 = 0.999$) between the fluorescence intensity of the R and S telomeres with a slope of 38.6. The calibration-corrected telomere fluorescence intensity was calculated as described (Herrera et al., 1999).

Images were recorded using a COHU CCD camera on a fluorescence microscope (Leitz DMRB; Leica). A mercury vapor lamp (CS 100W-2; Philips) was used as source. Images were captured using Leica Q-FISH software at 400 ms integration time in a linear acquisition mode to prevent over saturation of fluorescence intensity.

TFL-Telo software (gift from Dr. Lansdorp), was used to quantify the fluorescence intensity of telomeres from at least 15 metaphases or fusions of each data point. The images from littermate wild-type, PARP-1$^{+/-}$, and PARP-1$^{-/-}$ metaphases were captured on the same day, in parallel, and blindly. All the images from the MEF were captured in a 3 d period after the hybridization.

Flow-FISH. Fresh BM cells, splenocytes, and primary MEFs from littermate wild-type, PARP-1$^{+/-}$, and PARP-1$^{-/-}$ mice were prepared as described (Herrera et al., 1999). Flow-FISH hybridization was performed as described (Rufer et al., 1998). To normalize Flow-FISH data, two mouse leukemia cell lines (LY-R and LY-S, described above) were used as internal controls in each experiment. The telomere fluorescence of at least 2.000 cells gated at G1-G0 cell cycle stage was measured using a flow cytometer (EPICS XL; Beckman Coulter) with the SYSTEM 2 software.

TRF analysis. Fresh BM cells, splenocytes, and MEFs from wild-type, PARP-1$^{+/-}$, and PARP-1$^{-/-}$ littermate mice were isolated as described above and TRF analysis was done as described in Blasco et al. (1997).

G-strand overhang assay

The G-strand assay was performed as described (Samper et al., 2000), with minor modifications. MEFs from several pairs of wild-type and PARP-1$^{-/-}$ littermates were included in restriction analysis grade agarose plugs following instructions provided by the manufacturer (Bio-Rad Laboratories). After overnight digestion in LDS buffer (1% LDS, 100 mM EDTA, pH 8.0, and 10 mM Tris, pH 8.0), the plugs were digested with either 0, 40, or 100 U of mung bean nuclease for 15 min. Then the plugs were digested with MboI overnight and run in a pulse field gel electrophoresis as described (Blasco et al., 1997). The sequential in-gel hybridizations in native and denaturing conditions to visualize G-strand overhangs and telomeres, respectively, were carried out as described previously (Samper et al., 2000). Quantification of the G-strand overhang radioactive signals was carried out using a phosphoimager (STORM 860; Molecular Dynamics) and the software provided by the manufacturer. These values were corrected by the TRF signal in denaturing gel conditions.

Telomerase assay

S-100 extracts were prepared from wild-type, PARP-1$^{+/-}$, and PARP-1$^{-/-}$ primary MEF cultures, and a modified version of the TRAP assay was used to measure telomerase activity (Blasco et al., 1996). An internal control for PCR efficiency, IC, was included (TRAPeze kit Oncor).

Yeast two-hybrid assay

mTert cDNA was fused to the GAL 4 DNA binding domain of the pGBT8 vector (Hannon and Bartel, 1995). The human PARP-1 protein was fused to the GAL 4 activation domain of the pGAD424 vector. The host strain HF7c (Feilotter et al., 1994) was transformed using LiAC conventional transformation. The interacting proteins CDK4 and p16 were used as positive control.

We thank Rosa Serrano and Elisa Santos for mouse care and genotyping.

E. Samper is supported by a predoctoral fellowship from the regional government of Madrid (CAM), F. Goytisolo is supported by a postdoctoral fellowship from the CAM. M.A. Blasco's laboratory is funded by The Swiss Bridge Award 2000, by the Ministry of Science and Technology (PM97-0133), Spain, CAM 08.1/0030/98, the European Union (EURATOM/991/0201, FIGH-CT-1999-00002, FIS5-1999-00055), and by the Department

of Immunology and Oncology (DIO). The DIO is funded by the Spanish Council for Scientific Research and by Amersham Pharmacia Biotech. G. de Murcia laboratory is funded by Association pour la Recherche contre le Cancer, La Ligue contre le Cancer, Electricité de France, and Commissariat à l´Energie Atomique.

Submitted: 12 March 2001
Revised: 23 May 2001
Accepted: 31 May 2001

References

Alexander, P., and Z.B. Mikulski. 1961. Mouse lymphoma cells with different radiosensitivities. *Nature.* 192:572–577.

Ariumi, Y., M. Masutani, T.D. Copeland, T. Mimori, T. Sugimura, K. Shimotohno, K. Ueda, M. Hatanaka, and M. Noda. 1999. Suppression of the poly(ADP-ribose) polymerase activity by DNA-dependent protein kinase in vitro. *Oncogene.* 18:4616–4625.

Autexier, C., and C.W. Greider. 1996. Telomerase and cancer: revisiting the telomere hypothesis. *Trends Biochem.* 21:387–391.

Bailey, S.M., J. Meyne, D.J. Chen, A. Kurimasa, G.C. Li, B.E. Lehnert, and E.H. Goodwin. 1999. DNA double-strand break repair proteins are required to cap the ends of mammalian chromosomes. *Proc. Natl. Acad. Sci. USA.* 96: 14899–14904.

Beneke, R., C. Geisen, B. Zevnik, T. Bauch, W.U. Müller, J.H. Kupper, and T. Moroy. 2000. DNA excision repair and DNA damage-induced apoptosis are linked to poly(ADP-ribosyl)ation but have different requirements for p53. *Mol. Cell. Biol.* 20:6695–6703.

Bianchi, A. and T. de Lange. 1999. Ku binds telomeric DNA in vitro. *J. Biol. Chem.* 274:21223–21227.

Blackburn, E.H. 1991. Structure and function of telomeres. *Nature.* 350:569–573.

Blasco, M. A., M. Rizen, C.W. Greider, and D. Hanahan. 1996. Differential regulation of telomerase activity and telomerase RNA during multi-stage tumorigenesis. *Nat. Genet.* 12:200–204.

Blasco, M.A., H.-W. Lee, P. Hande, E. Samper, P. Lansdorp, R. DePinho, and C.W. Greider. 1997. Telomere shortening and tumor formation by mouse cells lacking telomerase RNA. *Cell.* 91:25–34.

Boulton, S.J., and S.P. Jackson. 1996. Identification of a *Saccharomyces cerevisiae* Ku80 homolog: roles in DNA double strand break rejoining and in telomeric maintenance. *Nucleic Acids Res.* 24:4639–4648.

Bürkle, A., V. Schreiber, F. Dantzer, J. Oliver, C. Niedergang, G. de Murcia, and J. Ménissier-de Murcia. 2000. Biological significance of poly (ADP-ribosyl)ation reactions: molecular and genetic approaches. Gilbert de Murcia and Sydney Shall, editors. Oxford University Press, Oxford, UK. 80–124.

d'Adda di Fagagna, F., M.P. Hande, W.-M. Tong, P.M. Lansdorp, Z.-Q. Wang, and S.P. Jackson. 1999. Functions of poly(ADP-ribose)polymerase in controlling telomere length and chromosomal stability. *Nat. Genet.* 23:76–80.

D'Amours, D., M. Germain, K. Orth, V.M. Dixit, and G.G. Poirier. 1998. Proteolysis of poly(ADP-ribose) polymerase by caspase 3: kinetics of cleavage of mono(ADP-ribosyl)ated and DNA-bound substrates. *Radiat. Res.* 150:3–10.

D'Amours, D., S. Desnoyers, I. D'Silva, and G.G. Poirier. 1999. Poly(ADP-ribosyl)ation reactions in the regulation of nuclear functions. *Biochem. J.* 342: 249–268.

Dantzer, F., H.P. Nasheuer, J.L. Vonesch, G. de Murcia, and J. Menissier-de Murcia. 1998. Functional association of poly(ADP-ribose) polymerase with DNA polymerase alpha-primase complex: a link between DNA strand break detection and DNA replication. *Nucleic Acids Res.* 26:1891–1898.

Dantzer, F., G. de la Rubia, J. Menissier-de Murcia, Z. Hostomsky, G. de Murcia, and V. Schreiber. 2000. Base excision repair is impaired in mammalian cells lacking the poly(ADP-ribose) polymerase-1. *Biochemistry.* 39:7559–7569.

de Lange, T. 1995. Telomere dynamics and genome instability in human cancer. *In* Telomeres. E. Blackbrun and C. Greider, editors. Cold Spring Harbor Press, Cold Spring Harbor, NY. 265–293.

Feilotter, H.E., G.J. Hannon, C.J. Ruddell, and D. Beach. 1994. Construction of an improved host strain for two hybrid screening. *Nucleic Acids Res.* 22: 1502–1503.

Galande, S., and T. Kohwi-Shigematsu. 1999. Poly(ADP-ribose) polymerase and Ku autoantigen form a complex and synergistically bind to matrix attachment sequences. *J. Biol. Chem.* 274:20521–20528.

Goytisolo, F., E. Samper, J. Martín-Caballero, P. Finnon, E. Herrera, J.M. Flores, S.D. Bouffler, and M.A. Blasco. 2000. Short telomeres result in organismal hypersensitivity to ionizing radiation in mammals. *J. Exp. Med.* 192:1625–1636.

Goytisolo, F., E. Samper, S. Edmonson, G.E. Taccioli, M.A. Blasco. 2001. Absence of DNA-PKcs in mice results in anaphase bridges and in increased telomeric fusions with normal telomere length and G-strand overhang. *Mol. Cell. Biol.* 21:3642–3651.

Greider, C.W. 1996. Telomere length regulation. *Annu. Rev. Biochem.* 65:337–365.

Griffith, J.D., L. Comeau, S. Rosenfield, R.M. Stansel, A. Bianchi, H. Moss, and T. de Lange. 1999. Mammalian telomeres end in a large duplex loop. *Cell.* 97:503–514.

Hande, P., E. Samper, P. Lansdorp, and M.A. Blasco. 1999. Telomere length dynamics in cultured cells from normal and telomerase null mice. *J. Cell Biol.* 144:589–601.

Hannon, G. and P. Bartel. 1995. Identification of interacting proteins using the two-hybrid system. *Methods Mol. Cell. Biol.* 5:289–297.

Herrera, E., E. Samper, J. Martín-Caballero, J.M. Flores, H.-W. Lee, and M.A. Blasco. 1999. Disease states associated to telomerase deficiency appear earlier in mice with short telomeres. *EMBO J.* 18:2950–2960.

Hsu, H.-L., D. Gilley, E. Backburn, and D.J. Chen. 1999. Ku is associated with the telomere in mammals. *Proc. Natl. Acad. Sci. USA.* 96:12454–12458.

Hsu, H.-L., D. Gilley, S.A. Galande, M.P. Hande, B. Allen, S.-H. Kim, G.C. Li, J. Campisi, T. Kowhi-Shigematsu, and D.J. Chen. 2000. Ku acts in a unique way at the mammalian telomere to prevent end joining. *Genes Dev.* 14: 2807–2812.

Jeggo, P.A. 1998. DNA repair: PARP - another guardian angel?. *Curr. Biol.* 8:49–51.

Lee, H.-W., M.A. Blasco, G.J. Gottlieb, J.W. Horner, C.W. Greider, and R.A. DePinho. 1998. Essential role of mouse telomerase in highly proliferative organs. *Nature.* 392:569–574.

Martin, S.G., T. Laroche, N. Suka, M. Grunstein, and S.M. Gasser. 1999. Relocalization of telomeric Ku and SIR proteins in response to DNA double-strand breaks. *Cell.* 97:621–633.

Martín-Rivera, L., E. Herrera, J.P. Albar, and M.A. Blasco. 1998. Expression of mouse telomerase catalytic subunit in embryos and adult tissues. *Proc. Natl. Acad. Sci. USA.* 95:10471–10476.

Masson, M., C. Niedergang, V. Schreiber, J. Ménissier-de Murcia, and G. de Murcia. 1998. XRCC1 is specifically associated with poly(ADP-ribose) polymerase and negatively regulates its activity following DNA damage. *Mol. Cell. Biol.* 18:3563–3571.

Matsutani, M., T. Nozaki, E. Nishiyama, T. Shimokawa, Y. Tachi, H. Suzuki, H. Nakagama, K. Wakabayashi, and M. Sugimura. 1999. Function of poly(ADP-ribose) polymerase in response to DNA damage: gene-disruption study in mice. *Mol. Cell. Biochem.* 193:14.

McClintock, B. 1941. The stability of broken ends of chromosomes in *Zea mays*. *Genetics.* 26:234–282.

McClintock, B. 1942. The fusion of broken ends of chromosomes following nuclear fusion. *Proc. Natl. Acad. Sci. USA.* 28:458–464.

McIlrath, J., S. Bouffler, E. Samper, A. Cuthbert, A. Wojcik, I. Szumiel, P.E. Bryant, A.C. Riches, A. Thompson, M.A. Blasco, R.F. Newbold, and P. Slijepcevic. 2001. Telomere length anormalities in mammalian radiosensitive cells. *Cancer Res.* 61:912–915.

Menissier-de Murcia, J., M. Molinete, G. Gradwohl, F. Simonin, and G. de Murcia. 1989. Zinc-binding domain of poly(ADP-ribose)polymerase participates in the recognition of single strand breaks on DNA. *J. Mol. Biol.* 210:229–233.

Menissier-de Murcia, J.M., C. Niedergang, C. Trucco, M. Ricoul, B. Dutrillaux, M. Mark, F.J. Oliver, M. Masson, A. Dierich, M. LeMeur, C. Walztinger, P. Chambon, and G. de Murcia. 1997. Requirement of poly(ADP-ribose) polymerase in recovery from DNA damage in mice and in cells. *Proc. Natl. Acad. Sci. USA.* 94:7303–7307.

Mills, K.D., D.A. Sinclair, and L. Guarente. 1999. MEC1-dependent redistribution of the Sir3 silencing protein from telomeres to DNA double-strand breaks. *Cell.* 97:609–620.

Morrison, C., G.C. Smith, L. Stingl, S.P. Jackson, E.F. Wagner, and Z.Q. Wang. 1997. Genetic interaction between PARP and DNA-PK in V(D)J recombination and tumorigenesis. *Nat. Genet.* 17:479.

Nugent, C.I., and V. Lundblad. 1998. The telomerase reverse transcriptase: components and regulation. *Genes Dev.* 12:1073–1085.

Nugent, C.I., G. Bosco, L.O. Ross, S.K. Evans, A.P. Salinger, J.K. Moore, J.E. Haber, and V. Lundblad. 1998. Telomere maintenance is dependent on activities required for end repair of double-strand breaks. *Curr. Biol.* 8:657–660.

Oei, S.L., J. Griesenbeck, M. Schweiger, V. Babich, A. Kropotov, and N. Tomilin. 1997. Interaction of the transcription factor YY1 with human poly(ADP-ribosyl) transferase. *Biochem. Biophys. Res. Commun.* 240:108–111.

Pieper, A.A., A. Verma, J. Zhang, and S. Snyder. 1999. Poly(ADP-ribose) polymerase, nitric oxide and cell death. *Trends Biochem.* 20:171–181.

Plaza, S., M. Aumercier, M. Bailly, C. Dozier, and S. Saule. 1999. Involvement of poly(ADP-ribose)-polymerase in the Pax-6 gene regulation in neuroretina. *Oncogene*. 18:1041–1051.

Poirier, G.G., G. de Murcia, J. Jongstra-Bilen, C. Niedergang, and P. Mandel. 1982. Poly(ADP-ribosyl)ation of polynucleosomes cause relaxation of chromatin structure. *Proc. Natl. Acad. Sci. USA.* 79:3423–3427.

Rufer, N., W. Dragowska, G. Thornbury, E. Roosnek, and P.M. Lansdorp. 1998. Telomere length dynamics in human lymphocyte subpopulations measured by flow cytometry. *Nat. Biotechnol.* 16:743–747.

Ruscetti, T., B.E. Lehnert, J. Halbrook, H. Le Trong, M.F. Hoekstra, D.J. Chen, and S.R. Peterson. 1998. Stimulation of the DNA-dependent protein kinase by poly (ADP-ribose) polymerase. *J. Biol. Chem.* 273:14461–14467.

Samper, E., F. Goytisolo, P. Slijepcevic, P. van Buul, and M.A. Blasco. 2000. Mammalian Ku86 prevents telomeric fusions independently of the length of TTAGGG repeats and the G-strand overhang. *EMBO Rep.* 1:244–252.

Shall, S., and G. de Murcia. 2000. Poly(ADP-ribose) polymerase-1: what have we learned from the deficient mouse model? *Mutat. Res.* 460:1–15.

Serrano, M., G.J. Hannon, and D. Beach. 1993. A new regulatory motif in cell-cycle control causing specific inhibition of cyclin D/CDK4. *Nature.* 366: 704–707.

Simbulan-Rosenthal, C.M., D.S. Rosenthal, H. Hilz, R. Hickey, L. Malkas, N. Applegren, Y. Wu, G. Bers, and M.E. Smulson. 1996. The expression of poly(ADP-ribose)polymerase during differentiation linked DNA replication reveals that it is a component of the multiprotein DNA replication complex. *Biochemistry*. 35:11622–1633.

Smith, S., and T. de Lange. 2000. Tankyrase promotes telomere elongation in human cells. *Curr. Biol.* 10:1299–1302.

Smith, S., I. Girlat, A. Schmitt, and T. de Lange. 1999. Tankyrase, a poly(ADP-ribose) polymerase at human telomeres. *Science.* 282:1484–1487.

Trucco, C., J. Oliver, G. de Murcia, and J. Ménissier de Murcia. 1998. DNA repair defect in poly(ADP-ribose)polymerase-deficient cell lines. *Nucleic Acids Res.* 26:2644–2649.

van Steensel, B., and T. de Lange. 1997. Control of telomere length by human telomeric protein TRF1. *Nature.* 385:740–743.

van Steensel, B., A. Smogorzewska, and T. de Lange. 1998. TRF2 protects human telomeres from end-to-end fusions. *Cell.* 92:401–413.

Wang, Z.-Q., B. Auer, L. Stingl, H. Berhammer, D. Haidacher, M. Schweiger, and E.W. Wagner. 1995. Mice lacking ADPRT and poly(ADP-ribosyl)ation develop normally but are susceptible to skin disease. *Genes Dev.* 9:509–520.

Wong, K.K., S. Chang, S.R. Weiler, S. Ganesan, J. Chaudhuri, C. Zhu, S.E. Artandi, K.L. Rudolph, G.J. Gottlieb, L. Chin, F.W. Alt, and R.A. DePinho. 2000. Telomere dysfunction impairs DNA repair and enhances sensitivity to ionizing radiation. *Nat. Genet.* 1:85–88.

Zhu, X.D., B. Kuster, M. Mann, J.H. Petrini, and T. de Lange. 2000. Cell-cycle-regulated association of RAD50/MRE11/NBS1 with TRF2 and human telomeres. *Nat. Genet.* 25:347-352.

Zijlmans, J.M., U.M. Martens, S. Poon, A.K. Raap, H.J. Tanke, R.K. Ward, and P.M. Lansdorp. 1997. Telomeres in the mouse have large inter-chromosomal variations in the number of T_2AG_3 repeats. *Proc. Natl. Acad. Sci. USA.* 94:7423–7428.